

Levitation by a dipole electric field

Ping-Rui Tsai¹, Hong-Yue Huang¹, Jih-Kang Hsieh¹, Yu-Ting Cheng¹, Ying-Pin Tsai², Cheng-Wei Lai³, Yu-Hsuan Kao⁴, Wen-Chi Chen⁵, Fu-Li Hsiao², Po-Heng Lin³ and Tzay-Ming Hong^{1*}

¹*Department of Physics, National Tsing Hua University, Hsinchu, Taiwan 30013, ROC*

²*Institute of Photonics, National Changhua University of Education, Changhua, Taiwan 50007, ROC*

³*Department of Chemistry, National Chung Hsing University, Taichung, Taiwan 40200, ROC*

⁴*Department of Color and Illumination Technology,*

National Taiwan University of Science and Technology, Taipei, Taiwan 106335, ROC and

⁵*Institute of Photonics Technologies, National Tsing Hua University, Hsinchu, Taiwan 30013, ROC*

(Dated: January 3, 2024)

The phenomenon of floating can be fascinating in any field, with its presence seen in art, films, and scientific research. This phenomenon is a captivating and pertinent subject with practical applications, such as Penning traps for antimatter confinement and Ion traps as essential architectures for quantum computing models. In our project, we reproduced the 1893 water bridge experiment using glycerol and first observed that lump-like macroscopic dipole moments can undergo near-periodic oscillations that exhibit floating effects and do not need classical bridge form. By combining experimental analysis, neural networks, investigation of Kelvin force generated by the Finite element method, and exploration of discharging, we gain insights into the mechanisms of motion. Our discovery has overturned the previous impression of a bridge floating in the water, leading to a deeper understanding of the new trap mechanism under strong electric fields with a single pair of electrodes.

In 1893, the British engineer William Armstrong conducted the elegant water bridge experiment, which is considered a representative example of changing the properties of matter to counteract weight[1]. When we apply a high voltage of about kilovolts to a pair of opposite electrodes immersed in two beakers filled with pure deionized water, a water bridge can form at the millimeter to centimeter scale, which can be floating[2]. This phenomenon also occurs in numerous polar dielectric liquids[3]. For nearly 130 years, Scientists aim to understand (1) the floating mechanism, (2) the characteristics of internal flow, and (3) the unique structure of WB. One prevailing theory considers surface tension and Kelvin force induced by Maxwell pressure as the main source to resist weight [3–5] and maintain the bridge’s contour. Although Raman spectroscopy [6] detects differences in spectroscopic signals between WB and water without the external electric field, X-ray analysis [7] does not reveal any ordered arrangement. However, MRI and PIV experiments identify a distinctive double-layer flow structure within WB [8, 9]. So far, no comprehensive theoretical framework is able to integrate all these experimental findings.

Here, we show new phenomenon has remained undiscovered for nearly 132 years, namely, levitating without the threads connect to both beakers. In other words, floating droplet without the “bridge” structure. Using glycerol (1.2 Pa·s) approximately 10,000 times more viscous than water (8.9×10^{-4} Pa·s) at room temperature, we observed levitating glycerol clusters (GC) capable of suspending without the need for a bridge structure, as depicted in Fig. 1(a). This new discovery provides a breakthrough in understanding the mechanisms behind the floating phenomena, shedding further light on WB. The detailed experimental procedures can be found in

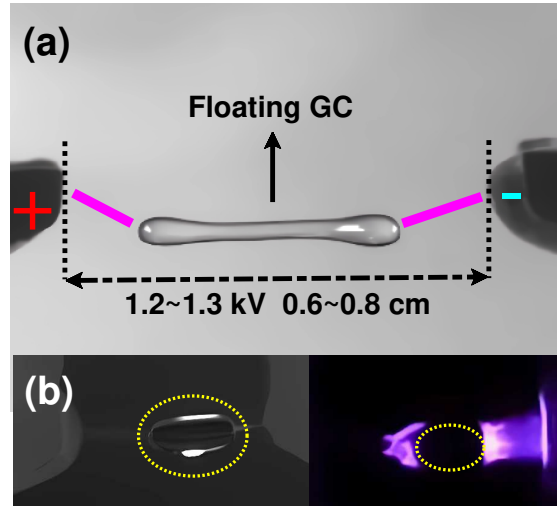


FIG. 1. (a) The GC is formed after the threads on both ends of bridge are broken. While floating in mid-air, GC not only performs extrusion and compression, but its center-of-mass also oscillates both horizontally and vertically, where purple lines denote the presence of plasma after GC is disconnected to beakers. (b) provide evidence of the purple blocks as plasma clusters, while the yellow dotted lines indicate the contour of GC. For live actions, consult SM Videos 1~2 for videos and 3 for plasma [10].

the Supplemental Material (SM)[10].

Our project explores three topics: 1. Trajectory of GC and vertical motion. 2. Plasma interaction and horizontal motion. 3. Levitation mechanism. Data were captured by a high-speed camera of 3000 fps and analyzed by Open CV [11] to track the trajectory of more than 14 sets of GC in order to find the patterns of their motion

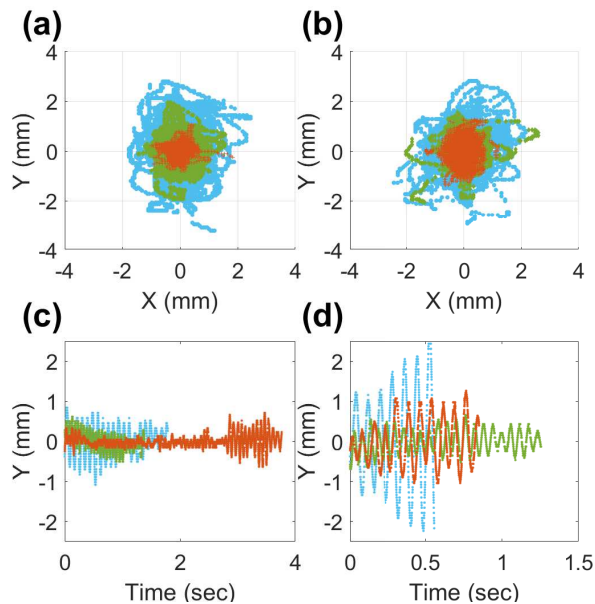


FIG. 2. The left and right plots, obtained by voltage $V=12000$ and 13000 V, exhibit similar features. The red, green, and blue lines represent results obtained by adjusting the distance between two spouts at 0.6 , 0.7 , and 0.8 cm. (a, b) show the distribution of GC trajectories, while (c, d) illustrate the oscillatory feature of its vertical position.

under six different conditions: the gap between beakers can be chosen between $L=0.6$, 0.7 and 0.8 cm, while there are two choices of voltages $V=12000$ and 13000 V. For detailed information regarding OpenCV, please refer to the SM [10].

In the early generation phase of GC, it demonstrates a process of fracturing from both sides, followed by compression and stretching in the vertical direction caused by external forces. Unlike conventional electric traps that require multiple pairs of precisely arranged electrodes [12, 13], GC levitation only makes use of one pair of electrodes in Fig. 1(a). As has been reported during the formation of WB [14], the plasma discharge is also observed when GC is disconnected to the beakers in Fig. 1(b).

The trajectories of GC in Fig. 2 show that it is not only confined to a finite range, but also oscillates in time during its lifetime of 0.1 to 1 s. In Fig. 2(a, b), we found that the motion trajectories were limited to an approximately elliptical range. In Fig. 2(c, d), we explored the oscillation behavior in the vertical direction Y.

To retrieve more features from the data in Fig. 2, we utilize Convolutional Neural Network (CNN) [15] and Pearson correlation (PCCs) to obtain Fig. 3(a, b). The CNN is a deep learning capable of extracting features. Here we develop a classifier to label the six conditions of GC samples based on the 11 features depicted in Fig. 3(a). In addition, we utilize a trained CNN that incorporates Gradient-weighted Class Activation Mapping (grad-CAM) [16]. This method allows us to trace back

the discriminative pathways for determining the conditions using the backward method [17]. By doing so, we can evaluate the 11 features that are most effective in determining the state to which a particular sample belongs. This helps us understand the primary sources of contribution from these features. The average grad-CAM for each condition is shown with a sample number of 9800. The notation of abbreviations is: ‘L / R’ for the left / right endpoint of GC, ‘C’ for the center point, and ‘L1, L2, R2, R1’ for the area of GC that is divided into four equal parts. The details of deep learning and grad-CAM see SM [10].

PCCs provide insights into the interdependence of various GC characteristics over time, and assess the correlation between two variables, quantifying the degree and direction of their association. Following the numerical labeling from Fig. 3(a), Fig. 3(b) indicates that the dynamics in the X and Y-directions are independent and derived from different mechanisms. However, the lack of significant dependence between L and R in the X-direction indicates that the impinge by plasma on one endpoint does not affect the motion of the other.

The vertical motion of GC in Fig. 2(c, d) clearly has nothing to do with the surface tension because it is an internal force. But during the formation of GC in Fig. 3(c), there still exist two thin threads that connect GC to the sprouts. If the surface tension indeed plays an important role for WB in the presence of uniform electric field [4], it ought to strengthen the effective spring constant for the vertical motion of GC in Fig. 3(c) and decrease the amplitude in Fig. 2(c, d). The fact that their amplitudes are roughly equal further casts doubt on the theory.

From the typical configuration of GC in Fig. 4(a), we believe the GC on both ends imply induced charges, the Coulomb attraction between which and electrodes engages in a tug of force with the surface tension. The temporal variation of $S1$ and $S2$, defined as the length of left and right stretching arms. This phenomenon is reminiscent of the Taylor cone before the formation of WB [18, 19]. The center-of-mass of GC also oscillates horizontally, as shown in Fig. 4(b, c). One possible physical explanation is that, say, if initially the left end of GC accumulates more charges than the right, the net Coulomb force will move GC toward the left. Once the gap between GC and the left electrode is narrow enough, plasma discharge ensues and empties the induced charge on the left. This reverses the balance of Coulomb force and repeats the above processes toward the other direction.

In general, the rate of plasma discharge on the left and right of GC should be uncorrelated because they are determined by their corresponding gaps to the electrodes. However the correlation between $S1$ and $S2$ in Fig. 4(d). Surprisingly, all five intervals during the lifetime of GC exhibit a PCCs above 0.7 indicating high synchronicity. Another counter-intuitive finding is that the average length of GC, d , is found to decrease when we raise the electric field in Fig. 4(e). When the GC re-

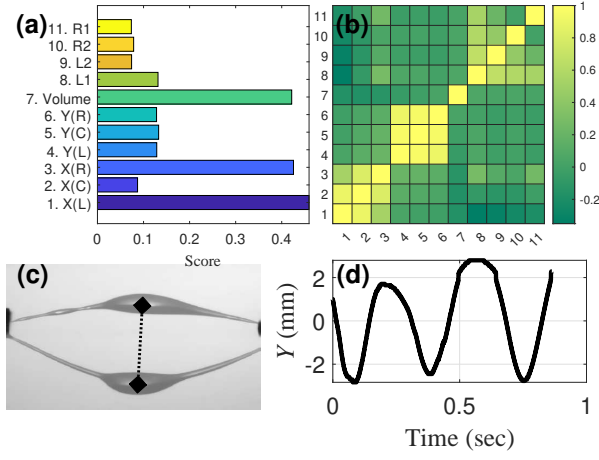


FIG. 3. (a) displays the use of grad-CAM to comprehend the significant features. It reveals that the total area and the characteristics of the two endpoints in the X-direction are among the top three highest-scoring features. (b) represents the similarity matrix of PCCs among the eleven features. (c,d) They represent the oscillation of GCs connected to threads in the Y direction. The oscillation range is between $-2 \sim 2$ mm, similar to GCs without threads. Additionally, during the oscillation, the threads are not solely affected by floating forces, indicating an additional degree of freedom unrelated to weight resistance by surface tension.

mains attached to one sprout and attempts to reach the other beaker, the plasma discharge bombardment pushes it back. Consequently, a stronger electric field leads to a shorter cone, ultimately causing it to shed its remaining thread and become completely disconnected.

Now, let's quantify the levitation mechanism from the classical Pellat experiment [20], which is based on the Kelvin force. First we define the polarization density P as

$$\vec{P} = D\vec{p} = (\epsilon - \epsilon_0)\vec{E} \quad (1)$$

where D represents the number of dipoles with moment \vec{p} per unit volume, from the polarization constitutive law, where ϵ_0 and ϵ are vacuum and dielectric permittivity. These dipole moments experience a force generated by a nonuniform electric field, called the Kelvin polarization force density: [3, 21–23]

$$\vec{F}_{\text{Kelvin}} = \vec{P} \cdot \nabla \vec{E} \quad (2)$$

Substituting Eq. (1) into (2), we can obtain

$$\vec{F}_{\text{Kelvin}} = \frac{1}{2}\epsilon_0(\epsilon_r - 1)\nabla(E^2). \quad (3)$$

Since the air undergoes electrical breakdown at 3 kV/cm [24], we witnessed the presence of plasma in the gaps between GC and the sprout of beaker, as confirmed in Fig. 2(e,f) and Supplementary Videos 4~8 [10]. As a result, the main electric potential will fall across GC. We conducted simulations using COMSOL Multiphysics

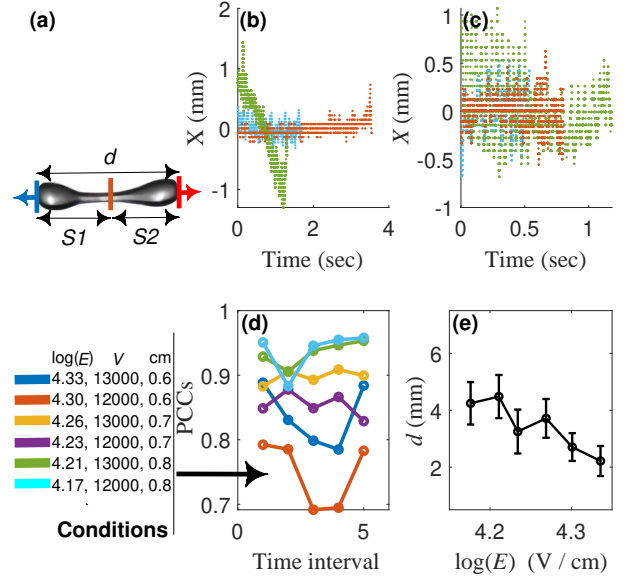


FIG. 4. (a) displays prominent GC of the Taylor cones at both ends. Blue/red arrows represent charges driven by positive/negative electrode beakers, and 'd' indicates the centroid distance between the two Taylor cone. (b-c) illustrate GC's centroid displacement in the X direction over time, consistent with the condition in Fig. 3 (a, b). (d) shows PCCs of stretching amounts of the two Taylor cones under different electric fields. All PCCs values above 0.7 indicate approximately equal and synchronized charging and discharging mechanisms, preventing significant X-direction displacement. (e) explores the influence of average length 'd' under different electric fields, the stronger the electric field, the shorter the length.

with the Finite Element Method, as detailed see SM[10]. In our simulations, we explored the conditions with the minimum electric field for $V=12000$ V and $L=0.8$ cm, and defined the amplitude as the standard error of oscillation, about 0.5 mm in the Y-direction. Utilizing Eq. (3), we determined the Y-directional Kelvin force density (KFDY), of which the simulation results of three scenarios are presented in Fig. 5(a), the ratio (RT) of the Kelvin force to the weight of GC is $O(2)$.

After applying fast Fourier transform (FFT) to the Y oscillations of all GCs conditions in Fig. 3, we observe two main peaks in Fig. 5(b). Under the same conditions as those used in the COMSOL simulation, namely 12000 V and 0.8 cm, the observed periods are approximately 6×10^{-2} and 3.3×10^{-4} seconds. Based on Fig. 2(d) where there are approximately 7 oscillation cycles within 0.5 seconds, we conclude that 6×10^{-2} s is the true period, while the shorter one arises from noises. Let's plug the period in the net force $M\ddot{y} = -M(2\pi/T)^2y$ where M is the mass of GC and the amplitude $y \approx -0.5$ mm. This yields an experimental estimation for the RT at 1.5.

The curiosity to achieve floating is not limited to the realm of art, science fictions, and films, but can actually be realized in lab experiments. The latter include elec-

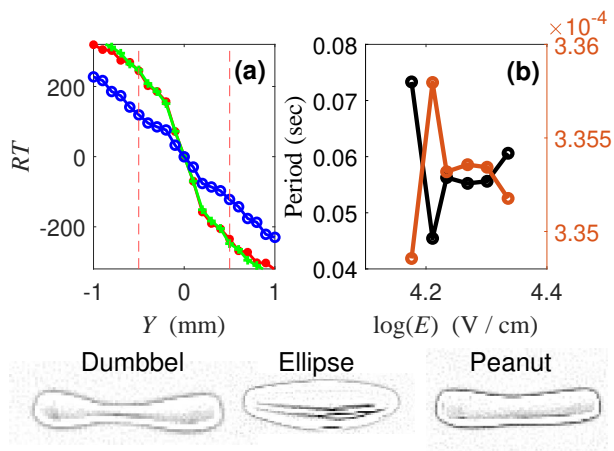


FIG. 5. (a) depicts the RT of three commonly observed GC shapes, with geometric descriptions provided below. The blue circles represent the Peanut (P) shape, while the red and green describe the Dumbbell (D) and Ellipse (E) overlap. The two red vertical dashed lines represent the position of one standard error of 0.5. (b) illustrates the results of double-period oscillations under various conditions in the Y -direction when subjected to FFT analysis.

trostatic levitation as in the famous Millikan’s oil drop experiment, magnetic levitation [25], optical levitation [26], acoustic levitation [27], and electro spray setup due to the Coulomb force effects [28]. Compared to current trapping methods like the Penning trap for anti-matter confinement and the various ion traps for quantum computing [29, 30], our setup makes use of only one pair of electrodes. The key to our GC confinement is a build-in stability - a combination of plasma discharge and interactions between dipole moments and trapping field. The discovery of GC not only opens up investigations into their peculiar phenomena, but also presents a new direction for the creation of simple potential wells in polar substances.

From Fig. 2, we clearly observed GC to oscillate periodically in the vertical direction within the survival time, indicating a reproducible and clear feat of floating. We specifically compared this motion of GC to that of its precursor, i.e., the classic phenomenon of WB in Fig. 3(c). The presence of GC represents a new direction in the field of EHD- relying on plasma to continuously connect GC and form a conducting channel that causes most of the voltage drop to be at across GC. This is crucial to increasing the electric field and its resulting Kelvin force density experienced by GC. This concept is distinct from the theory for WB, which claims that both surface tension and dielectric tension (equivalent to Kelvin force) contribute equally. Without connections to both beakers, surface tension becomes an internal force and obviously cannot contribute to levitating GC. Next, we demonstrated how to effectively trap GC in the horizontal direction, focusing on its interaction with the plasma in Fig. 5. Finally,

we delved into the mechanism behind levitation and examined the role of Kelvin force in Fig. 5.

The ratio between the Kelvin force and the weight of GC is experimentally determined to be about 1.5, in contrast to the numerical prediction of $O(2)$. We believe there are two factors that contribute to this discrepancy. The first derives from the internal electric field generated by the positive and negative ion charges accumulated respectively at the Taylor cone and polarization charges on opposite ends of GC[28], see Supplementary Video 9[10]. Since the simulation did not include such an effect, this field will reduce the predicted electric field inside the GC.

The second factor regards the interaction between plasma and the glycerin surface that we believe will influence the air’s conductivity. Supplementary Videos 5 and 6[10] clearly show that the trajectory of plasma will adjust its orientation and always point towards the GC as the latter oscillates vertically. In the mean time, we also noticed that there can be multiple trajectories of plasma, as opposed to just a single trajectory in COMSOL simulation.

We propose that the GC represents a simpler version of WB without the complications that arise from the bridge’s more frequent time-shifting morphology and complex internal flows. Furthermore, by tailoring the size of GC through the setup and employing relevant optical detection, we can gain a better understanding of its internal properties, unravel possible new chemical bonding, and explore the impact of high-voltage electricity on the internal state of fluids and soft materials, For example, it was previously mentioned that water was subjected to pulse laser influence, and the existence of the liquid crystal phase was detected within femtosecond [31].

Similar to all trap setups [32], increasing the lifetime of GC is crucial to gain wider applications and deeper insights. This requires clarifying details such as thermal effects [18, 33] and the plasma discharge [34] that may trigger internal flows for the droplet. These factors are likely responsible for the millimeter-scale oscillation that remains in the Y -direction in spite of the fact that the restoring force surpasses weight by three orders of magnitude. It worth mentioning that we did not observe the equivalent of GC in water. What happened was that the water column immediately broke into several droplets when WB became detached to both beakers due to thermal agitations. Since the surface tension coefficient of water is roughly equal to that of glycerol, we suspect this prominence of Rayleigh-Plateau instability in water column can be ascribed to its four orders more viscous.

Utilizing advanced graph neural networks (GNN) [35] to structure GC as a graph will be helpful to learn more behaviors. Another future work may be to check whether the liquid-liquid transition asserted by Fuchs *et al.* [36] also exists in GC. This research direction may provide a deeper understanding of the similarities and differences between GC and WB, and their unique properties.

- * ming@phys.nthu.edu.tw
- [1] Armstrong, W. Electrical phenomena the newcastle literary and philosophical society. *The Electrical Engineer*. **10** pp. 153 (1893)
 - [2] Fuchs, E., Gatterer, K., Holler, G. & Woisetschläger, J. Dynamics of the floating water bridge. *Journal Of Physics D: Applied Physics*. **41**, 185502 (2008)
 - [3] Woisetschläger, J., Wexler, A., Holler, G., Eisenhut, M., Gatterer, K. & Fuchs, E. Horizontal bridges in polar dielectric liquids. *Experiments In Fluids*. **52** pp. 193-205 (2012)
 - [4] Aerov, A. Why the water bridge does not collapse. *Physical Review E*. **84**, 036314 (2011)
 - [5] Namin, R., Lindi, S., Amjadi, A., Jafari, N. & Irajizad, P. Experimental investigation of the stability of the floating water bridge. *Physical Review E*. **88**, 033019 (2013)
 - [6] Ponterio, R., Pochylski, M., Aliotta, F., Vasi, C., Fontanella, M. & Saija, F. Raman scattering measurements on a floating water bridge. *Journal Of Physics D: Applied Physics*. **43**, 175405 (2010)
 - [7] Skinner, L., Benmore, C., Shyam, B., Weber, J. & Parise, J. Structure of the floating water bridge and water in an electric field. *Proceedings Of The National Academy Of Sciences*. **109**, 16463-16468 (2012)
 - [8] Wexler, A., Drusová, S., Fuchs, E., Woisetschläger, J., Reiter, G., Fuchsjäger, M. & Reiter, U. Magnetic resonance imaging of flow and mass transfer in electrohydrodynamic liquid bridges. *Journal Of Visualization*. **20** pp. 97-110 (2017)
 - [9] Tsai, P., Lai, C., Cheng, Y., Huang, C., Tsai, C., Lee, Y., Hao, H. & Hong, T. Evidence for spontaneous arrangement of two-way flow in water bridge via particle image velocimetry. *ArXiv Preprint arXiv:2004.04899*. (2020)
 - [10] Supplemental material.
 - [11] Names Module of Open CV. (<https://scikit-image.org/docs/stable/api/skimage.measure.html>,2000)
 - [12] Kielpinski, D., Monroe, C. & Wineland, D. Architecture for a large-scale ion-trap quantum computer. *Nature*. **417**, 709-711 (2002)
 - [13] Brown, L. & Gabrielse, G. Geonium theory: Physics of a single electron or ion in a Penning trap. *Reviews Of Modern Physics*. **58**, 233 (1986)
 - [14] Krbal, M., Stepanek, J., Wasserbauer, V., Orsagova, J. & Sumec, S. Floating water bridge phenomenon high voltage laboratory experiments. *2017 18th International Scientific Conference On Electric Power Engineering (EPE)*. pp. 1-4 (2017)
 - [15] Gu, J., Wang, Z., Kuen, J., Ma, L., Shahroudy, A., Shuai, B., Liu, T., Wang, X., Wang, G., Cai, J. & Others Recent advances in convolutional neural networks. *Pattern Recognition*. **77** pp. 354-377 (2018)
 - [16] Selvaraju, R., Cogswell, M., Das, A., Vedantam, R., Parikh, D. & Batra, D. Grad-cam: Visual explanations from deep networks via gradient-based localization. *Proceedings Of The IEEE International Conference On Computer Vision*. pp. 618-626 (2017)
 - [17] Shrikumar, A., Greenside, P. & Kundaje, A. Learning important features through propagating activation differences. *International Conference On Machine Learning*. pp. 3145-3153 (2017)
 - [18] Fuchs, E., Gatterer, K., Holler, G. & Woisetschläger, J. Dynamics of the floating water bridge. *Journal Of Physics D: Applied Physics*. **41**, 185502 (2008)
 - [19] Skinner, L., Benmore, C., Shyam, B., Weber, J. & Parise, J. Structure of the floating water bridge and water in an electric field. *Proceedings Of The National Academy Of Sciences*. **109**, 16463-16468 (2012)
 - [20] Pegourie, B., and J-M. Picchiottino. "Pellet ablation theory and experiments." *Plasma physics and controlled fusion* 35.SB (1993): B157.
 - [21] Fano, Robert M., Lan Jen Chu, and Richard B. Adler. *Electromagnetic fields, energy, and forces*. Taylor & Francis, 1963.
 - [22] Peng, Yanhong, et al. A review on electrohydrodynamic (EHD) pump. *Micromachines* **14.2**, 321 (2023)
 - [23] Haus, Hermann A., and James R. Melcher. *Electromagnetic fields and energy*. **107**. Englewood Cliffs: Prentice Hall, 1989.
 - [24] Tupikin, A. V., et al. "Combined optical and electrical discharge in air flow." *AIP Conference Proceedings*. **2288**. No. 1. AIP Publishing, 2020.
 - [25] Simon, M. & Geim, A. Diamagnetic levitation: Flying frogs and floating magnets. *Journal Of Applied Physics*. **87**, 6200-6204 (2000)
 - [26] Moffitt, J., Chemla, Y., Smith, S. & Bustamante, C. Recent advances in optical tweezers. *Annu. Rev. Biochem.* **77** pp. 205-228 (2008)
 - [27] Falkovich, Gregory, et al. "Floater clustering in a standing wave." *Nature* 435.7045 (2005): 1045-1046.
 - [28] Agostinho, L. L. F., et al. "Reverse movement and coalescence of water microdroplets in electrohydrodynamic atomization." *Physical Review E* 84.2 (2011): 026317.
 - [29] Häffner, H., Roos, C. & Blatt, R. Quantum computing with trapped ions. *Physics Reports*. **469**, 155-203 (2008)
 - [30] Andresen, G., Bertsche, W., Boston, A., Bowe, P., Cesar, C., Chapman, S., Charlton, M., Chartier, M., Deutsch, A., Fajans, J. & Others Antimatter plasmas in a multipole trap for antihydrogen. *Physical Review Letters*. **98**, 023402 (2007)
 - [31] Kim, Kyung Hwan, et al. "Anisotropic x-ray scattering of transiently oriented water." *Physical Review Letters* 125.7 (2020): 076002.
 - [32] Cheng, T., Lindner, M. & Sen, M. Implications of a matter-antimatter mass asymmetry in Penning-trap experiments. *ArXiv Preprint arXiv:2210.10819*. (2022)
 - [33] Singh, B., Rajendran, L., Giarra, M., Vlachos, P. & Bane, S. Measurement of the flow field induced by a spark plasma using particle image velocimetry. *Experiments In Fluids*. **59** pp. 1-15 (2018)
 - [34] Kumar, H., Bera, S., Dasgupta, S., Sood, A., Dasgupta, C. & Maiti, P. Dipole alignment of water molecules flowing through a carbon nanotube. *Physical Review B*. **107**, 165402 (2023)
 - [35] Sanchez-Gonzalez, A., Godwin, J., Pfaff, T., Ying, R., Leskovec, J. & Battaglia, P. Learning to simulate complex physics with graph networks. *International Conference On Machine Learning*. pp. 8459-8468 (2020)
 - [36] Fuchs, E., Woisetschläger, J., Wexler, A., Pecnik, R. & Vitiello, G. Electrically Induced Liquid-Liquid Phase Transition in a Floating Water Bridge Identified by Refractive Index Variations. *Water*. **13**, 602 (2021)